

ROVER: Robust Loop Closure Verification with Trajectory Prior in Repetitive Environments

Jingwen Yu^{1,2}, Jiayi Yang³, Anjun Hu⁴, Jiankun Wang⁴, Ping Tan¹, and Hong Zhang², *Life Fellow, IEEE*

Abstract—Loop closure detection is important for simultaneous localization and mapping (SLAM), which associates current observations with historical keyframes, achieving drift correction and global relocalization. However, a falsely detected loop can be fatal, and this is especially difficult in repetitive environments where appearance-based features fail due to the high similarity. Therefore, verification of a loop closure is a critical step in avoiding false positive detections. Existing works in loop closure verification predominantly focus on learning invariant appearance features, neglecting the prior knowledge of the robot’s spatial-temporal motion cue, i.e., trajectory. In this letter, we propose ROVER, a loop closure verification method that leverages the historical trajectory as a prior constraint to reject false loops in challenging repetitive environments. For each loop candidate, it is first used to estimate the robot trajectory with pose-graph optimization. This trajectory is then submitted to a scoring scheme that assesses its compliance with the trajectory without the loop, which we refer to as the trajectory prior, to determine if the loop candidate should be accepted. Benchmark comparisons and real-world experiments demonstrate the effectiveness of the proposed method. Furthermore, we integrate ROVER into state-of-the-art SLAM systems to verify its robustness and efficiency. Our source code and self-collected dataset are available at <https://github.com/jarvisyiw/ROVER>.

Index Terms—Loop Closure, SLAM, Localization

I. INTRODUCTION

With SLAM advancing into the “robust-perception age” [3], its deployment in unconstrained environments demands higher levels of robustness and reliability. Loop closure detection (LCD) has proven to be highly critical in ensuring global map consistency [4], achieving submap merging [5], and recovery from tracking failure [6]. LCD identifies the associations between a pair of previously visited and current locations, subsequently incorporating the constraint into the SLAM back-end for optimization. However, incorrect loop closure constraints can have fatal consequences in robot state estimation, leading to its failure. The typical LCD pipeline, which contains a retrieval and a verification stage, is shown in Fig. 2. In the retrieval stage, compact global descriptors are extracted and compared to find the top n candidates for the verification stage, which robustly rejects false candidates. While existing works mainly focus on the retrieval stage, aiming to increase the recall, the

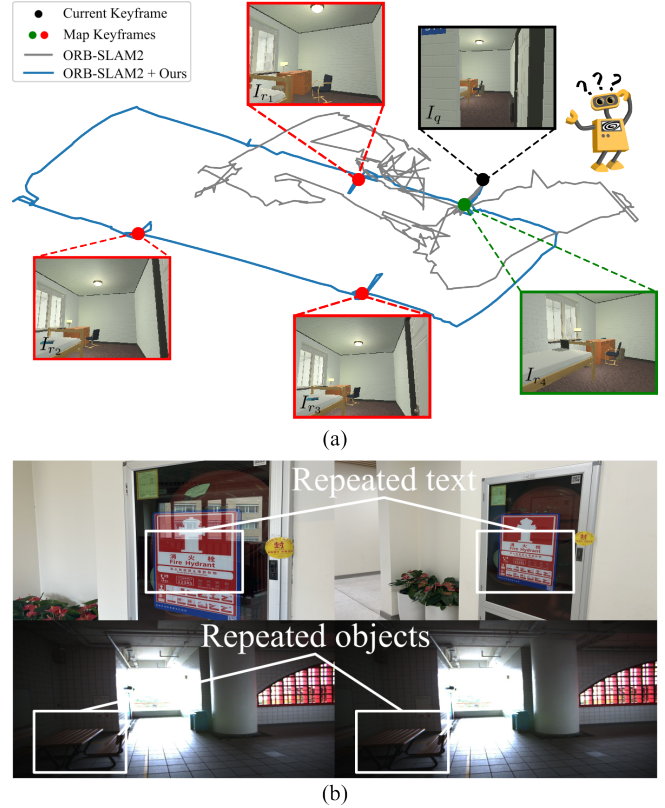


Fig. 1: (a) A **typical repetitive scenario** where a SLAM algorithm (e.g., ORB-SLAM2) fails in appearance-based loop verification. I_q is the current keyframe (i.e., query image) used to detect loop closures, I_{r_i} are the retrieved images among the map keyframes (i.e., reference database). Due to the visual similarity, geometric verification cannot disambiguate between true positives (green dot) and false positives (red dot). However, the proposed method incorporates the trajectory cues to reject false loops robustly. (b) **Typical scenes where text [1] and semantics-based methods [2] fail**. The upper row of Fig. 1 (b) shows a false loop with repeated text, and the lower row contains a false loop with repeated objects.

verification stage, which ensures the precision, is scarcely studied. In this letter, we focus on the verification stage, i.e., loop closure verification (LCV), which aims to robustly reject the false loop closures.

Currently, loop closure verification is achieved primarily through geometric verification (GV), which has been exhaustively benchmarked in GV-Bench [7]. The existing challenges for GV that have been reported include repetitive patterns, illumination changes, dynamic scene changes, and

¹ CKS Robotics Institute, Hong Kong University of Science and Technology, Hong Kong SAR, China (jyubt@connect.ust.hk)

² Shenzhen Key Laboratory of Robotics and Computer Vision, Southern University of Science and Technology, Shenzhen, China

³ The University of Tokyo, Tokyo, Japan

⁴ Department of Electronic and Electrical Engineering, Southern University of Science and Technology, China

* Corresponding author: Hong Zhang (hzhang@sustech.edu.cn)

large viewpoint variations. Existing works focus on rejecting false loop closures via invariant visual features as described in Sec. II-B, predominantly relying on the similarity in visual appearance, neglecting the historical motion cue of the robot. Appearance-based methods suffer from severe perceptual aliasing in repetitive environments, as shown in Fig. 1.

This paper aims to address the challenge of loop closure verification in repetitive environments. We propose a novel method independent of appearance features that leverages the robot’s historical trajectory. Since the proposed method does not rely on sensor measurements, it is inherently sensor-agnostic and can be integrated into any SLAM system, including visual SLAM, LiDAR SLAM, Radar SLAM, etc. However, in this letter, for clarity of presentation, we focus on demonstrating the effectiveness of the proposed method within a visual SLAM framework.

We draw inspiration from Vertigo [8], which observes that a subset of false-positive loops within a given set of loop candidates can be identified by analyzing the changes in residual error as the candidate loops are selectively introduced to the pose graph optimization (PGO). In practical SLAM, however, loop candidates are detected sequentially, necessitating that LCV considers one loop at a time. In contrast to [8], our work proposes to examine the changes in the robot’s trajectory before and after incorporating a loop constraint into PGO. Intuitively, adding a correct loop to PGO, the change of the robot trajectory would be continuous and graceful; while adding a false loop, the change would be chaotic and catastrophic [9]. By leveraging this prior knowledge in LCV, the challenge in repetitive environments can be largely circumvented. Our contributions can be summarized as follows:

- 1) **A novel loop closure verification method** that leverages the trajectory prior rather than relying on appearance.
- 2) **A scoring scheme** that evaluates the change between two trajectories as the confidence of loop candidates.
- 3) **Tight integration into SLAM systems** to demonstrate the proposed method’s robustness through extensive experiments on public datasets and real-world experiments.

The rest of the paper is organized as follows. Section II reviews the relevant literature. Section III overviews the proposed system and presents the core technical contribution. Section IV demonstrates the experimental results, followed by a conclusion in Section V.

II. RELATED WORKS

A. Localization and Mapping in Repetitive Environments

Existing visual simultaneous localization and mapping (SLAM) systems depend on either sparse local features [4] or photometric consistency [10], and their LCD component faces challenges in environments with a high degree of repetitive patterns, such as office buildings, warehouses, and underground parking lots. To address this challenge, various techniques can be employed, including artificial landmarks [11], magnetic fields (MF) [12], and radio frequency

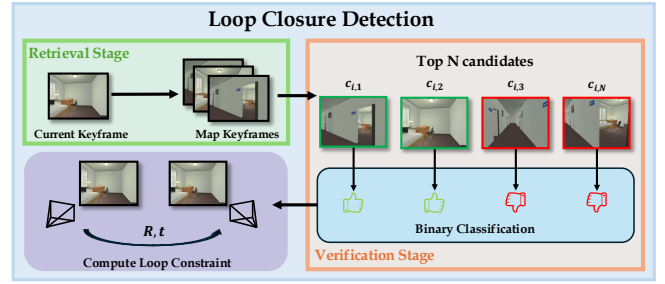


Fig. 2: **Two-stage Loop Closure Detection Pipeline.** i) Retrieval stage adopts image retrieval techniques to match historical keyframes. ii) Verification stage serves as a binary classifier that rejects the falsely detected loop candidates.

(RF) [13]. Moreover, [14] proposes to take advantage of the structure of the Manhattan environment prior to the topological mapping of warehouse scenes. These methods highly rely on environment modification, extra sensors, or environmental prior knowledge, leading to limited generalization ability and an increase in cost. In contrast, the proposed loop closure verification method seamlessly integrates with existing SLAM frameworks, as illustrated in Fig. 3, offering both flexibility and effectiveness for real-time autonomous robot navigation.

B. Loop Closure Verification

As shown in Fig. 2, the two-stage loop closure detection consists of a retrieval stage and a verification stage. Existing LCD methods mainly focus on the retrieval stage, either ignoring the verification stage or adopting a standard method for the verification stage, which is responsible for the rejection of falsely retrieved candidates. In this section, we review the existing solutions designed for LCV. Currently, geometric verification (GV) based on multiview geometry serves as the dominant solution to reject falsely detected loop candidates. Specifically, the epipolar constraint in two-view geometry is used to conduct RANSAC, and the number of inliers of local feature matches serves as an indication of positive likelihood. GV has recently been greatly enhanced by learning-based local feature techniques [15]–[17]. However, it still faces challenges in visually similar scenarios since the epipolar constraint fails due to repetitive patterns [7]. [2] targets rejecting the falsely detected loops with the assistance of a large language model (LLM). It first extracts the scene semantics (e.g., door numbers) and then uses a visual question and answer (VQA) model to generate a text description. Then it feeds the text description and tailored prompt to ChatGPT. It faces challenges caused by repeated semantic entities and scenes without textual information, as shown in Fig. 1(b). Moreover, it heavily relies on the reasoning ability of an LLM, which is not certifiable and struggles to achieve real-time performance.

As an alternative for addressing the challenges for LCV in repetitive environments, we propose a novel approach that utilizes information from the robot’s trajectory before and after PGO rather than relying on appearance information

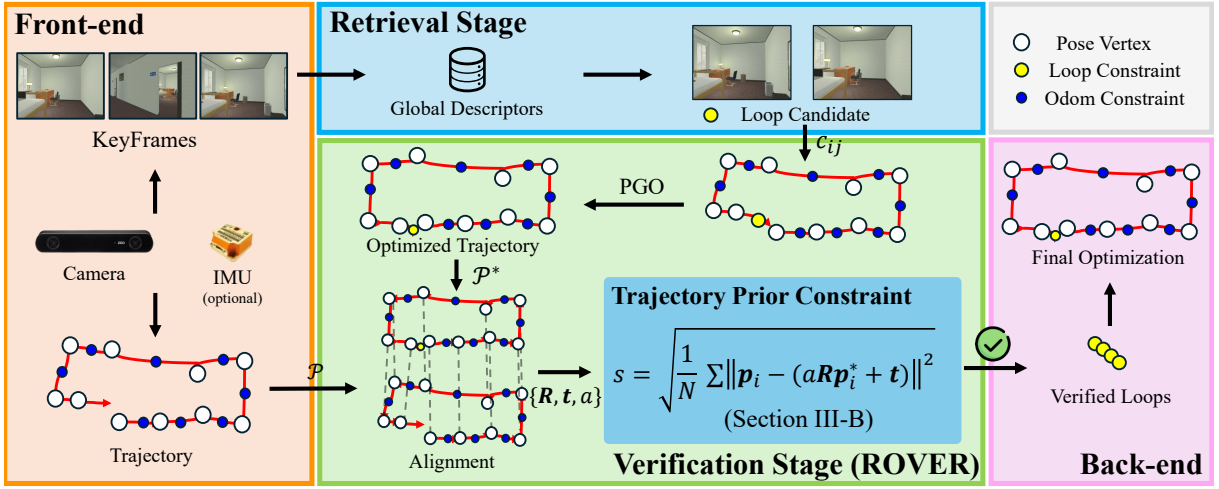


Fig. 3: **System overview** of a complete SLAM pipeline with proposed loop verification method. Our main contribution lies in the verification stage (as explained in Section III-C), which takes loop constraints from the retrieval stage and the estimated trajectory from the front-end to predict a confidence score for rejecting false loops. In the end, the verified loops are accepted for the final back-end optimization.

within the current view and the loop candidate. As a result, it can effectively avoid ambiguous scenarios in repetitive scenes while offering seamless integration with existing SLAM systems.

III. METHODOLOGY

This section presents our proposed ROVER by first defining the notations used. Section III-B overviews the system design as demonstrated in Fig. 3, followed by a detailed description of the trajectory prior constraint (TPC) in Section III-C. We further extend our work by integrating it into visual SLAM systems to validate its efficacy in Section III-D.

A. Notations

Throughout the paper, we denote the keyframe collected at the k -th time as \mathcal{F}_k . A rigid transform $\mathbf{x}_k = [\mathbf{R}_k | \mathbf{p}_k] \in SE(3)$ represents the pose of \mathcal{F}_k relative to \mathcal{F}_0 . A robot trajectory can be represented by a set of keyframe poses denoted as $\mathcal{X} = \{\mathbf{x}_i\}_n$. The translation part of the trajectory is denoted as $\mathcal{P} = \{\mathbf{p}_k | \mathbf{p}_k \in \mathbb{R}^3\}$. The pose graph $\mathcal{G} = (\mathcal{X}, \mathcal{U})$ consists of a set of nodes \mathcal{X} and a set of noisy relative measurements $\mathcal{U} = \{\mathbf{u}_{ij} | \mathbf{u}_{ij} \in SE(3)\}$ between \mathcal{F}_i and \mathcal{F}_j .

B. System Overview

The proposed pipeline is illustrated in Fig. 3, where ROVER serves as an intermediate layer between front-end estimation and back-end optimization. The proposed design follows the convention of the classical pose graph SLAM framework. Thus, it can be integrated into the SLAM system regardless of sensing modality. In this letter, we focus on the visual SLAM systems. The front-end odometry estimates the pose of keyframes $\{\mathcal{F}_i\}_n$, which produces \mathcal{X}_n and corresponding odometry constraints $\{c_{i,i+1}\}_{n-1}$ from relative measurements \mathcal{U}_n :

$$c_{i,i+1} = \|f(\mathbf{x}_i, \mathbf{u}_i) - \mathbf{x}_{i+1}\|_{\Sigma_i}^2. \quad (1)$$

The loop detection module detects the top k candidates for each keyframe, producing k loop candidates $\{\mathcal{F}_i, \mathcal{F}_j\}_k$. For each candidate, a relative pose \mathbf{u}_{ij} is estimated. Accordingly, a loop constraint c_{ij} is generated:

$$c_{ij} = \|f(\mathbf{x}_i, \mathbf{u}_{ij}) - \mathbf{x}_j\|_{\Lambda_{ij}}^2. \quad (2)$$

The classical PGO is formulated as follows:

$$\begin{aligned} \mathcal{X}^* = \operatorname{argmin}_{\mathcal{X}} & \underbrace{\sum_i^n \|f(\mathbf{x}_i, \mathbf{u}_i) - \mathbf{x}_{i+1}\|_{\Sigma_i}^2}_{\text{Odometry Constraints}} \\ & + \underbrace{\sum_{ij}^k \|f(\mathbf{x}_i, \mathbf{u}_{ij}) - \mathbf{x}_j\|_{\Lambda_{ij}}^2}_{\text{Loop Constraints}}. \end{aligned} \quad (3)$$

ROVER takes \mathcal{X} and loop constraint c_{ij} as input, and predicts a loop verification score s_{ij} based on the trajectory prior constraint (TPC) described in Section III-C, which can be injected into the PGO formulation seamlessly:

$$\begin{aligned} \mathcal{X}^* = \operatorname{argmin}_{\mathcal{X}} & \sum_i^n \|f(\mathbf{x}_i, \mathbf{u}_i) - \mathbf{x}_{i+1}\|_{\Sigma_i}^2 \\ & + \|\Psi(s_{ij}) * (f(\mathbf{x}_i, \mathbf{u}_{ij}) - \mathbf{x}_j)\|_{\Lambda_{ij}}^2. \end{aligned} \quad (4)$$

Note that our proposed system verifies the detected loop individually in a sequential manner as described in Equation (4). Loops are verified by thresholding the probability $\Psi: \mathbb{R} \rightarrow \{0, 1\}$. If a loop closure candidate fails to pass the threshold, it is rejected for further back-end optimization. In this way, ROVER bridges the front-end odometry estimation and back-end optimization, building a robust SLAM framework.

C. Trajectory Prior Constraint

The trajectory inherently contains historical motion cues, which can serve as a strong prior for loop verification to enhance the precision of LCD. As discussed earlier in Section I,

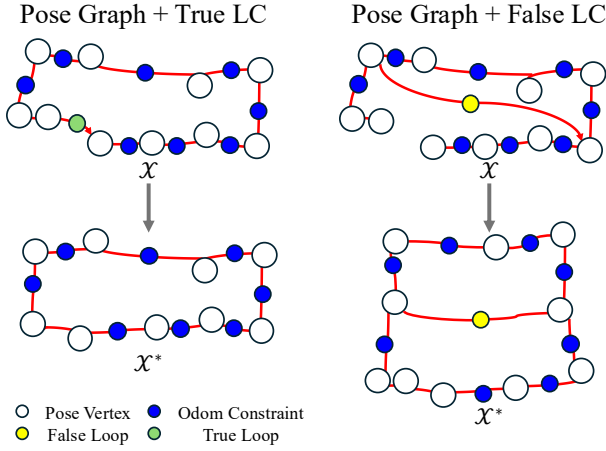


Fig. 4: **Illustrative example of TPC.** Adding a true loop to PGO would result in a continuous and graceful change, as shown on the left-hand side, while a false loop is more likely to result in a chaotic change, as shown on the right.

the key intuition is that a valid loop closure should correct drift, resulting in a graceful change rather than distorting the entire trajectory into a chaotic shape, as illustrated in Fig. 4. To this end, we propose measuring the change of the trajectory before and after PGO, i.e., between \mathcal{X} and \mathcal{X}^* , under the assumption that the loop constraint c_{ij} holds true. The proposed scoring scheme is in two folds: i) align \mathcal{X} and \mathcal{X}^* based on the coherent timestamps, and ii) compute the change score of two aligned trajectories. For the alignment of two trajectories, using only the translational components is sufficient, as discussed in [18]. Therefore, we take \mathcal{P} and \mathcal{P}^* , which represents the translational part of trajectories of \mathcal{X} and \mathcal{X}^* , respectively. We adopt [19] for alignment by finding the rigid $SIM(3)$ transform $\mathcal{S}^* = \{\mathbf{R}, \mathbf{t}, a\}$ that satisfies:

$$\mathcal{S}^* = \underset{\mathcal{S}}{\operatorname{argmin}} \sum_{i=0}^{N-1} \|\mathbf{p}_i - a\mathbf{R}\mathbf{p}_i^* - \mathbf{t}\|^2. \quad (5)$$

Then, the Euclidean distance between the aligned trajectories is taken as the confidence s_{ij} for verification:

$$s_{ij} = \sqrt{\frac{1}{N} \sum_{i=0}^{N-1} \|\mathbf{p}_i - (a\mathbf{R}\mathbf{p}_i^* + \mathbf{t})\|^2}, \quad (6)$$

where $\{\mathbf{R}, \mathbf{t}, a\} \in \mathcal{S}^*$. The complete algorithm pipeline can be summarized in Algorithm 1. A pose graph \mathcal{G} can be constructed from the front-end of SLAM following Equation (3) along with a loop candidate constraint c_{ij} . Notably, the proposed method is designed for sequential input, i.e., loop candidates are verified one by one, a scenario where PGO methods that require batch input typically fail. Finally, the verification is accomplished by first aligning the translational part of the trajectories \mathcal{P} and \mathcal{P}^* using Equation (5) and predicting the score using Equation (6).

D. Integration into SLAM Systems

LCD is closely tied to SLAM systems, as variations in keyframe selection strategies can significantly impact loop

Algorithm 1 Loop Verification based on TPC

```

1: Notation: Pose Graph  $\mathcal{G}$ , Loop Candidate  $c_{ij}$ 
2: Input:  $\mathcal{X}$  and  $c_{ij}$ 
3: Output: Predicted label  $\{0, 1\}$  for  $c_{ij}$ 
4: Initialize  $\mathcal{G} \leftarrow$  Front-end
5:  $\mathcal{X}^* \leftarrow PGO(\mathcal{G}, c_{ij})$  // Equation (3)
6: if PGO Converge then
7:    $\{\mathcal{P}, \mathcal{P}^*\} \leftarrow \{\mathcal{X}, \mathcal{X}^*\}$ 
8:    $\mathcal{S}^* = TrajAlign(\mathcal{P}, \mathcal{P}^*)$  // Equation (5)
9:    $s_{ij} = ComputeScore(\mathcal{P}, \mathcal{P}^*, \mathcal{S}^*)$  // Equation (6)
10:  if  $\Psi(s_{ij}) == 1$  then
11:    return 1
12:  end if
13: end if
14: return 0

```

detection results. To highlight the effectiveness of ROVER, we evaluate it alongside real-time SLAM systems. ORB-SLAM2 and VINS-Fusion are selected as baselines for experiments, representing state-of-the-art (SOTA) visual SLAM and visual-inertial SLAM approaches, respectively. While the proposed method is in general compatible with any sensor modality, this section focuses on typical visual SLAM systems as examples. ORB-SLAM2 represents the keyframe-based visual SLAM approach, featuring a dedicated *LoopClosing* thread for loop retrieval, verification, and correction. Similarly, VINS-Fusion includes a *LoopFusion* thread that functions in a manner analogous to ORB-SLAM2's *LoopClosing* thread. Here, we use the *LoopClosing* thread as an example to demonstrate the integration of ROVER into the SLAM pipeline in Algorithm 2. When a new valid

Algorithm 2 *LoopClosing* Thread with ROVER

```

1: Notation: Map Keyframes  $\mathcal{K} = \{\mathcal{F}_k\}$ , Latest Keyframe  $\mathcal{F}_i$ 
2: Initialize:  $\mathcal{F}_i \leftarrow$  Tracking Thread
3: while  $\mathcal{K} \neq \emptyset$  do
4:   if CheckNewKeyFrame( $\mathcal{F}_i$ ) then
5:      $\mathcal{F}_j \leftarrow DetectLoop(\mathcal{F}_i)$ 
6:     if  $0 \leq j < i$  then
7:        $c_{ij}, n_{matches} \leftarrow ComputeSim3(\mathcal{F}_i, \mathcal{F}_j)$ 
8:       if  $n_{matches} \geq 40$  then
9:          $s_{ij} \leftarrow ROVER(\mathcal{G}, c_{ij})$ 
10:        if  $\Psi(s_{ij}) == 1$  then
11:          CorrectLoop()
12:        end if
13:      end if
14:    end if
15:  end if
16: end while

```

keyframe \mathcal{F}_i arrives, DBow2 is employed to retrieve the closest historical keyframe \mathcal{F}_j . Then, *ComputeSim3* returns a loop constraint c_{ij} by estimating the relative pose from local feature matching, if \mathcal{F}_i and \mathcal{F}_j pass the GV. In default

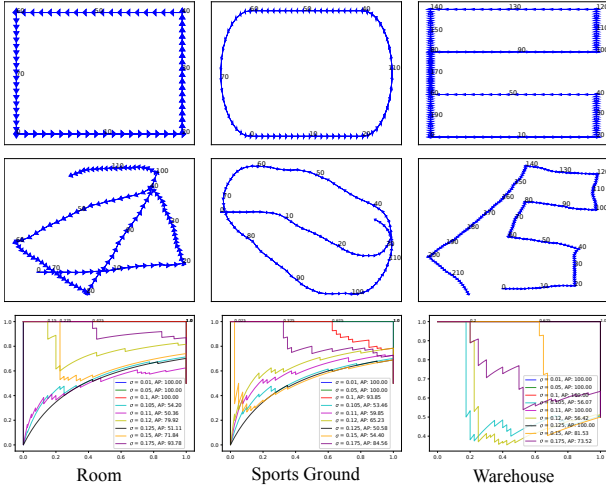


Fig. 5: **Proof-of-Concept Experiment.** Top row: Ground truth trajectory. Middle row: Simulated odometry with noise level $\sigma = 0.1$. Bottom row: Precision-Recall Curve of the proposed method under different noise levels $\sigma \in [0.01, 0.175]$.

ORB-SLAM2, the threshold for GV is set to 40 inliers. The loop is further verified by ROVER given the pose graph \mathcal{G} and loop constraint c_{ij} . Finally, the verified loop will be used for loop correction. The *LoopFusion* thread of VINS-Fusion follows a similar logic as described above in Algorithm 2. For implementation details, we refer readers to our open-source code.

IV. EXPERIMENTAL RESULTS

In this section, we first introduce a set of proof-of-concept experiments to demonstrate the rationale of the foundation design of our approach in Fig. 5. Three scenarios are simulated with different levels of Gaussian noise imposed on the ground truth to mimic drift in odometry estimation. Datasets and metrics used for experiments are described in Section IV-A, including a self-collected one with a customized hardware design. Subsequently, we conduct comprehensive experiments from two perspectives:

- 1) Loop closure verification (Section IV-B): We compare the proposed work with GV baselines, which are normally employed as the verification stage of LCD. Moreover, SOTA visual place recognition methods are benchmarked in reference to the LCD’s retrieval stage.
- 2) Localization accuracy (Section IV-C): We evaluate the localization accuracy by integrating the proposed method with visual SLAM baselines to demonstrate the practical efficacy.

Finally, we conclude this section by discussing the existing limitations and potential directions for future improvement in Section IV-D.

A. Datasets and Metrics

The core contribution of our work lies in developing a robust LCV method for SLAM in repetitive environments.

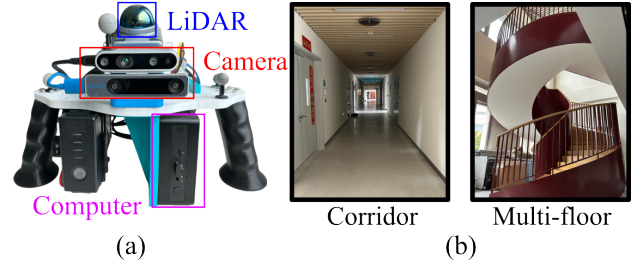


Fig. 6: (a) Our handheld device for collecting the Cross-floor dataset. (b) Snapshots of the Cross-floor dataset.

Although existing public datasets that focus on repetitive environments are limited, we managed to find three that contain repetitive scenes in common robots’ operation scenarios: the Hotel [2], Warehouse [20], and large-scale multi-floor Escalator [21]. To further evaluate the effectiveness of our approach, we collected a dataset in a typical indoor office building, referred to as Cross-floor.

1) *Public datasets*: The Hotel and the Warehouse datasets are collected in simulated environments. The Hotel dataset contains a monocular stream of two traverses over six hotel rooms on the same floor with similar appearances. In the Warehouse dataset, a logistic robot is used to collect the data, which does not contain revisits (i.e., true positive loops) as shown in Fig. 7. However, due to the high visual similarity between storage racks, false loops occur. The Escalator dataset is collected in the real world using a handheld device that moves across four levels of an indoor building for two rounds. As shown in the second row of Fig. 1(b), scenes with no text and repeated objects, which exist in the Escalator dataset, pose significant challenges for text- and semantics-inspired methods [1], [2].

2) *Self-collected dataset*: As demonstrated in Fig. 6, a customized hardware setup was built for data collection, comprising a Livox Mid360, Intel RealSense D435i, and Intel RealSense T265. Fast-LIO2 [34] was utilized to generate the ground truth trajectory. The dataset captures a typical repetitive scene characterized by long corridors and cross-floor traverses, where the layouts of different floors are highly similar. Notably, it can be challenging for humans to distinguish between the corridors without relying on text signs. However, as shown in the first row of Fig. 1(b), repeated text in the environment introduces difficulties for methods that heavily depend on scene text. To validate this observation, TextInPlace [27], which leverages scene text for reranking, is evaluated alongside appearance-only baselines.

3) *Metrics*: We evaluate the proposed method using task-specific metrics. For loop closure verification, the objective is to robustly determine true positives (TP) over all the retrieved loop candidates. We follow GV-Bench [7] to use maximum recall @100 precision (MR) and average precision (AP) as the evaluation metrics. MR represents the maximum percentage of true loops that can be identified while rejecting all the false samples. For the localization accuracy, the commonly used root mean square error (RMSE) of absolute

TABLE I: **Experiment results of loop closure verification.** Best and second best results are highlighted. The last column presents the average performance of all datasets. **MR** represents maximum recall @100 precision, **AP** stands for average precision. The results are rounded to two decimal places.

	Method	Hotel [2]		Warehouse [20]		Escalator [21]		Cross-floor		Average	
		AP	MR	AP	MR	AP	MR	AP	MR	AP	MR
Retrieval	DBoW [22]	99.18	37.37	88.72	<u>76.92</u>	91.03	5.38	97.08	18.43	94.00	34.53
	NetVLAD [23]	89.37	0.29	45.56	15.38	82.46	0.0	80.71	0.0	74.53	3.92
	MixVPR [24]	90.57	0.44	51.35	23.08	79.15	0.0	78.56	0.0	74.91	5.88
	AnyLoc [25]	90.49	0.0	44.77	15.38	80.58	0.0	75.53	0.0	72.84	3.85
	SALAD [26]	91.74	0.0	51.72	23.08	77.83	0.0	78.82	0.0	75.03	5.77
	TextInPlace [27]	95.23	0.0	44.83	0.0	89.04	0.0	86.30	0.16	78.85	0.04
Geometric Verification	ORB-NN [4]	99.55	61.38	90.18	<u>76.92</u>	95.55	32.31	96.61	36.85	95.47	51.87
	SIFT-NN [28]	98.88	36.12	87.32	<u>76.92</u>	94.08	26.92	96.41	17.64	94.17	39.40
	SIFT-LG [29]	98.85	13.44	87.67	69.23	98.03	63.85	96.88	46.61	95.36	48.28
	SP-SG [15]	95.24	2.58	<u>90.18</u>	<u>76.92</u>	94.34	37.69	97.01	17.95	94.19	33.78
	LoFTR [16]	98.79	48.24	86.80	<u>76.92</u>	<u>98.57</u>	62.31	<u>98.39</u>	45.83	95.06	50.41
	eLoFTR [30]	98.68	44.71	86.80	<u>76.92</u>	98.74	59.23	96.00	26.46	95.06	51.83
	DISK-LG [31]	99.43	33.33	86.63	61.54	97.17	53.85	98.23	<u>54.80</u>	95.37	50.88
	ALIKED-LG [32]	97.59	25.99	82.19	46.15	90.90	20.00	90.51	1.26	90.30	23.35
	DUST3R [33]	96.67	2.79	58.95	15.38	97.18	53.85	85.51	3.15	84.58	18.79
	MASt3R [17]	97.24	10.06	76.82	38.46	95.29	4.62	89.05	6.14	89.60	14.82
Vertigo [8]		97.36	0.00	44.83	0.00	89.04	0.00	86.28	0.00	79.38	0.00
ROVER (Ours)		99.68	78.12	100.00	100.00	97.77	<u>61.54</u>	99.23	88.03	99.25	87.39

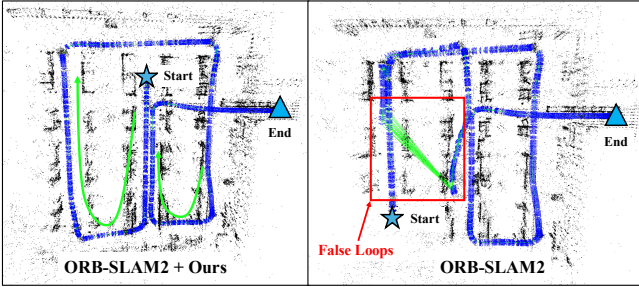


Fig. 7: **ORB-SLAM2's mapping result** w/ and w/o the proposed method of the Warehouse dataset. There are no revisits in the dataset. Thus, ORB-SLAM2 w/ the proposed method produces a more accurate reconstruction.

trajectory error (ATE) is adopted.

B. Experiments on Loop Closure Verification

To better mimic the online LCD process, keyframe-based visual odometry is used to generate a keyframe database for benchmarking over each dataset. We use VINS-Fusion [35], [36] for the Escalator and Cross-floor dataset, and a tailored ORB-SLAM2 (*LoopClosing* thread disabled) for the Hotel and Warehouse dataset. Loop candidates are generated by DBoW2 for verification, with their format structured as [7] and annotated manually. The experiment results in Table I are divided into three parts:

Retrieval: We use the Euclidean distance $d(\mathbf{v}_q, \mathbf{v}_r)$ as the verification score, where $\mathbf{v}_q, \mathbf{v}_r$ represent the global descriptors of query and database images, respectively. All the baselines, including the text-based two-stage VPR method TextInPlace [27], demonstrate significant limitations under

repetitive environments. It is also confirmed that the verification stage is a must for a robust LCD.

Geometric Verification: The number of RANSAC-filtered inlier matches is used as the verification score. We compare over different baselines of popular local feature matching, including 3D geometric foundation models like DUST3R [33] and MASt3R [17]. ROVER achieves robust performance across all datasets with the highest AP and MR. For the Escalator dataset, although the VINS-Fusion's odometry estimation is noisy and unstable, ROVER still achieves competitive performance compared to a costly semi-dense feature matcher LoFTR [16].

Ours vs. Vertigo: As highlighted in Section I, while Vertigo is designed to process a batch of loop candidates as input, it is inherently capable of handling a single loop candidate. As an outlier rejection method, it identifies outliers among inliers, a process different from LCV, where only one loop candidate is presented. In practice, Vertigo is conservative, often rejecting most candidates. This behavior stems from the fact that adding a true loop constraint to a pose graph, which initially relies solely on odometry, typically results in an increased residual error.

In conclusion, ROVER presents robust performance over the existing LCV methods in repetitive environments.

C. Experiments on Localization Accuracy

We integrate ROVER with ORB-SLAM2 and VINS-Fusion to evaluate the localization accuracy as shown in Table II. We compare the ATE over two settings: i) Visual Odometry (VO) and ii) SLAM. For ORB-SLAM2, VO denotes a tailored ORB-SLAM2 with *LoopClosing* thread disabled. For VINS-Fusion, *LoopFusion* thread is optional in the original implementation. We can see that the SLAM

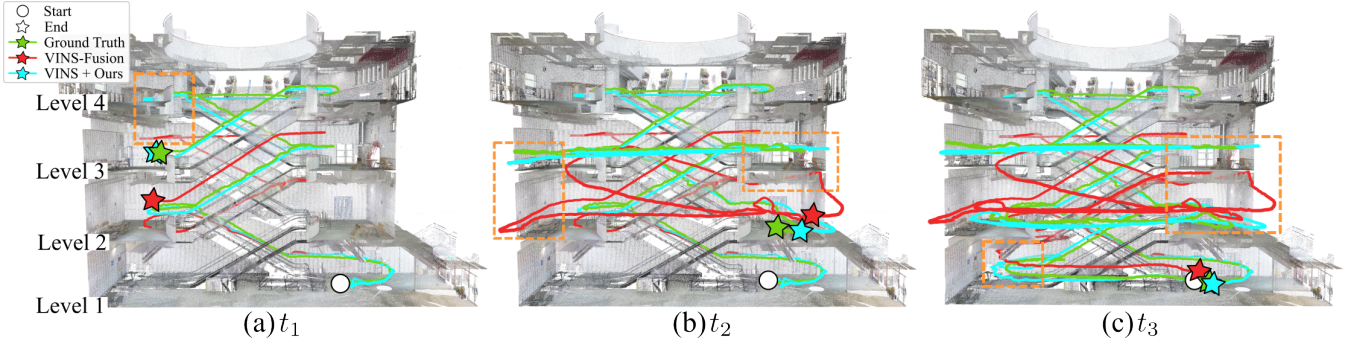


Fig. 8: **Trajectory comparison of the Escalator dataset.** The colored point cloud is used for visualization only.

TABLE II: The comparisons of the RMSE (meters) of ATE of SLAM systems w/ and w/o the proposed method. **Best** results are highlighted.

	Method	Hotel	Warehouse	Escalator	Cross-floor
VO	ORB-SLAM2	0.67	0.56	\times	\times
	VINS-Fusion	\times	\times	1.14	0.48
SLAM	ORB-SLAM2	2.17	15.50	\times	\times
	VINS-Fusion	\times	\times	2.49	1.99
	ORB-SLAM2 + Ours	0.11	0.56	\times	\times
	VINS-Fusion + Ours	\times	\times	1.00	0.40

systems w/o ROVER over all datasets exhibit huge errors due to the false positive (FP) loops caused by repetitive patterns in the scenes. However, ROVER is capable of rejecting those FPs to get a more accurate localization performance. In the Warehouse dataset, due to the absence of revisits, ORB-SLAM2 with ROVER achieves the identical result as VO. We also compare our approach with various Mono-SLAM algorithms, including learning-based methods, as shown in Fig. 9. The results demonstrate that repetitive scenes pose substantial challenges for learning-based algorithms as well.

In addition, we evaluate the real-time localization safety by measuring ATE once in a fixed time interval in Table III. We conducted the experiment over the Escalator dataset, where the whole traverse is divided into 5 evenly distributed intervals. At t_1 , t_2 , and t_3 , the VINS-Fusion shows significantly worse ATE compared to the ATE of the entire traverse at t_4 . For the three timestamps shown in the Fig. 8, VINS-Fusion estimates false localization across different floors, which can be fatal for robotic operations, depicting the deficiency of ATE evaluation over the complete traverse. Therefore, we propose to compute a temporal ATE (tATE):

$$tATE = \sqrt{1/k \sum e(\mathcal{T}_{t_i} - \mathcal{T}_{t_i}^{gt})^2}, t_i \in \{t_0, \dots, t_{k-1}\}, (7)$$

aiming to reflect the real-time localization safety.

D. Limitations and Future Work

As discussed in Fig. 5 and Section IV-B, the proposed method faces limitations due to the significant drift in the front-end's trajectory estimation, as it relies on the trajectory as prior knowledge. When integrating ROVER into SLAM

TABLE III: The comparisons of the RMSE (meters) of tATE of VINS-Fusion w/ and w/o the proposed method over the Escalator dataset. **Best** results are highlighted.

Method	t_0	t_1	t_2	t_3	t_4	tATE
VINS-Fusion (VO)	0.70	0.94	1.22	1.88	1.14	1.19
VINS-Fusion	0.70	4.73	3.89	2.90	2.49	3.05
VINS-Fusion + Ours	0.70	0.94	1.19	1.30	1.00	1.03

systems, a strict threshold is applied to ensure a conservative approach, accepting only a subset of true loop closures with high confidence. To mitigate this limitation, a potential solution involves dynamically adjusting the threshold by predicting uncertainty in odometry estimation. This would enable the relaxation of TPC based on the confidence level of state estimation. In other words, the confidence between the prior trajectory and loop closure should adapt to the uncertainty in odometry estimation. For future work, we plan to enhance the robustness of the ROVER by incorporating an online uncertainty estimator and collecting additional real-world datasets in scalable environments.

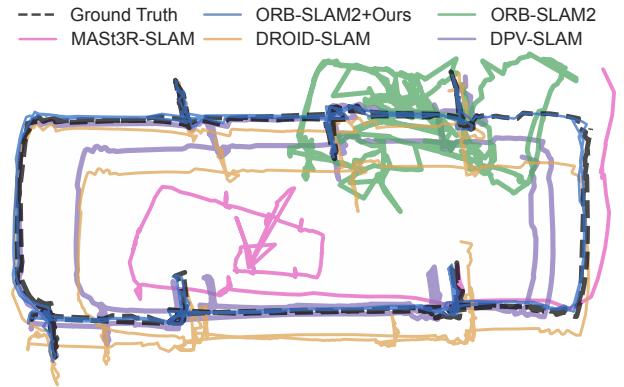


Fig. 9: **Trajectory comparison of the Hotel dataset.**

V. CONCLUSIONS

In this letter, we investigate the benefit of leveraging the trajectory prior constraint for LCV and propose ROVER, targeting repetitive environments. It achieves robust performance compared to the commonly adopted geometric verification methods, and it can be seamlessly integrated with

existing real-time SLAM frameworks. Extensive public and self-collected benchmark results validate the effectiveness and robustness of the proposed work. In the future, as discussed in Section IV-D, we plan to extend our framework by introducing dynamic uncertainty prediction in odometry estimation to further improve the robustness of our LCV method in scalable repetitive environments.

REFERENCES

- [1] T. Jin, X. Xu, Y. Yang, S. Yuan, T.-M. Nguyen, J. Li, and L. Xie, "Robust loop closure by textual cues in challenging environments," *IEEE Robot. Autom. Lett.*, 2024.
- [2] H. Li, S. Yu, S. Zhang, and G. Tan, "Resolving loop closure confusion in repetitive environments for visual slam through ai foundation models assistance," in *Proc. IEEE Int. Conf. Robot. Autom.* IEEE, 2024, pp. 6657–6663.
- [3] C. Cadena, L. Carlone, H. Carrillo, Y. Latif, D. Scaramuzza, J. Neira, I. Reid, and J. J. Leonard, "Past, present, and future of simultaneous localization and mapping: Toward the robust-perception age," *IEEE Trans. Robot.*, vol. 32, no. 6, pp. 1309–1332, 2016.
- [4] R. Mur-Artal and J. D. Tardós, "ORB-SLAM2: an open-source SLAM system for monocular, stereo and RGB-D cameras," *IEEE Trans. Robot.*, vol. 33, no. 5, pp. 1255–1262, 2017.
- [5] C. Campos, R. Elvira, J. J. G. Rodríguez, J. M. Montiel, and J. D. Tardós, "Orb-slam3: An accurate open-source library for visual, visual-inertial, and multimap slam," *IEEE Trans. Robot.*, vol. 37, no. 6, pp. 1874–1890, 2021.
- [6] W. Chen, L. Zhu, Y. Guan, C. R. Kube, and H. Zhang, "Submap-based pose-graph visual slam: A robust visual exploration and localization system," in *Proc. IEEE/RJS Int. Conf. Intell. Robots Syst.* IEEE, 2018, pp. 6851–6856.
- [7] J. Yu, H. Ye, J. Jiao, P. Tan, and H. Zhang, "Gv-bench: Benchmarking local feature matching for geometric verification of long-term loop closure detection," in *Proc. IEEE/RJS Int. Conf. Intell. Robots Syst.* IEEE, 2024, pp. 7922–7928.
- [8] N. Sünderhauf and P. Protzel, "Switchable constraints for robust pose graph slam," in *Proc. IEEE/RJS Int. Conf. Intell. Robots Syst.* IEEE, 2012, pp. 1879–1884.
- [9] Y. Latif, C. Cadena, and J. Neira, "Robust loop closing over time," in *Robot.: Sci. Syst.*, 2013, pp. 233–240.
- [10] H. Huang, H. Ye, Y. Sun, and M. Liu, "Monocular visual odometry using learned repeatability and description," in *Proc. IEEE Int. Conf. Robot. Autom.* IEEE, 2020, pp. 8913–8919.
- [11] S. Xu, Y. Dong, H. Wang, S. Wang, Y. Zhang, and B. He, "Bifocal-binocular visual slam system for repetitive large-scale environments," *IEEE Trans. Instrum. Meas.*, vol. 71, pp. 1–15, 2022.
- [12] Z. Wu, W. Wang, J. Zhang, Q. Lyu, H. Zhang, and D. Wang, "Global localization in repetitive and ambiguous environments," in *Proc. IEEE Int. Conf. Robot. Autom.* IEEE, 2023, pp. 12 374–12 380.
- [13] S. Zhang, S. Tang, W. Wang, T. Jiang, and Q. Zhang, "Conquering textureless with rf-referenced monocular vision for mav state estimation," in *Proc. IEEE Int. Conf. Robot. Autom.* IEEE, 2021, pp. 146–152.
- [14] S. S. Puligilla, S. Tourani, T. Vaidya, U. S. Parihar, R. K. Sarvadev-abhatla, and K. M. Krishna, "Topological mapping for manhattan-like repetitive environments," in *Proc. IEEE Int. Conf. Robot. Autom.* IEEE, 2020, pp. 6268–6274.
- [15] P.-E. Sarlin, D. DeTone, T. Malisiewicz, and A. Rabinovich, "Super-glue: Learning feature matching with graph neural networks," in *Proc. IEEE Conf. Comput. Vis. Pattern Recognit.*, 2020, pp. 4938–4947.
- [16] J. Sun, Z. Shen, Y. Wang, H. Bao, and X. Zhou, "Loftr: Detector-free local feature matching with transformers," in *Proc. IEEE Conf. Comput. Vis. Pattern Recognit.*, 2021, pp. 8922–8931.
- [17] V. Leroy, Y. Cabon, and J. Revaud, "Grounding image matching in 3d with mast3r," in *Proc. Eur. Conf. Comput. Vis.* Springer, 2024, pp. 71–91.
- [18] M. Salas, Y. Latif, I. D. Reid, and J. Montiel, "Trajectory alignment and evaluation in slam: Horns method vs alignment on the manifold," in *Robot.: Sci. and Sys. Workshop: The problem of mobile sensors.* sn, 2015, pp. 1–3.
- [19] S. Umeyama, "Least-squares estimation of transformation parameters between two point patterns," *IEEE Trans. Pattern Anal. Mach. Intell.*, vol. 13, no. 04, pp. 376–380, 1991.
- [20] H. Park, I. Lee, M. Kim, H. Park, and K. Joo, "A benchmark dataset for collaborative slam in service environments," *IEEE Robot. Autom. Lett.*, 2024.
- [21] J. Jiao, H. Wei, T. Hu, X. Hu, Y. Zhu, Z. He, J. Wu, J. Yu, X. Xie, H. Huang *et al.*, "Fusionportable: A multi-sensor campus-scene dataset for evaluation of localization and mapping accuracy on diverse platforms," in *Proc. IEEE/RJS Int. Conf. Intell. Robots Syst.* IEEE, 2022, pp. 3851–3856.
- [22] A. Angeli, D. Filliat, S. Doncieux, and J.-A. Meyer, "Fast and incremental method for loop-closure detection using bags of visual words," *IEEE Trans. Robot.*, vol. 24, no. 5, pp. 1027–1037, 2008.
- [23] R. Arandjelovic, P. Gronat, A. Torii, T. Pajdla, and J. Sivic, "Netvlad: Cnn architecture for weakly supervised place recognition," in *Proc. IEEE Conf. Comput. Vis. Pattern Recognit.*, 2016, pp. 5297–5307.
- [24] A. Ali-Bey, B. Chaib-Draa, and P. Giguere, "Mixvpr: Feature mixing for visual place recognition," in *Winter Conf. App. Comput. Vis.*, 2023, pp. 2998–3007.
- [25] N. Keetha, A. Mishra, J. Karhade, K. M. Jatavallabhula, S. Scherer, M. Krishna, and S. Garg, "Anyloc: Towards universal visual place recognition," *IEEE Robot. Autom. Lett.*, 2023.
- [26] S. Izquierdo and J. Civera, "Optimal transport aggregation for visual place recognition," in *Proc. IEEE Conf. Comput. Vis. Pattern Recognit.*, 2024, pp. 17 658–17 668.
- [27] H. Tao, B. Liu, C. Chen, T. Huang, H. Li, J. Cui, and H. Zhang, "Textinplace: Indoor visual place recognition in repetitive structures with scene text spotting and verification," in *Proc. IEEE/RJS Int. Conf. Intell. Robots Syst.* IEEE, 2025.
- [28] D. G. Lowe, "Object recognition from local scale-invariant features," in *Proc. IEEE Int. Conf. Comput. Vis.*, vol. 2, 1999, pp. 1150–1157.
- [29] P. Lindenberger, P.-E. Sarlin, and M. Pollefeys, "LightGlue: Local Feature Matching at Light Speed," in *Proc. IEEE Int. Conf. Comput. Vis.*, 2023.
- [30] Y. Wang, X. He, S. Peng, D. Tan, and X. Zhou, "Efficient LoFTR: Semi-dense local feature matching with sparse-like speed," in *Proc. IEEE Conf. Comput. Vis. Pattern Recognit.*, 2024.
- [31] M. Tyszkiewicz, P. Fua, and E. Trulls, "Disk: Learning local features with policy gradient," *Adv. Neural Inf. Process. Syst.*, vol. 33, 2020.
- [32] X. Zhao, X. Wu, W. Chen, P. C. Y. Chen, Q. Xu, and Z. Li, "Aliked: A lighter keypoint and descriptor extraction network via deformable transformation," *IEEE Trans. Instrum. Meas.*, vol. 72, pp. 1–16, 2023. [Online]. Available: <https://arxiv.org/pdf/2304.03608.pdf>
- [33] S. Wang, V. Leroy, Y. Cabon, B. Chidlovskii, and J. Revaud, "Dust3r: Geometric 3d vision made easy," in *Proc. IEEE Conf. Comput. Vis. Pattern Recognit.*, 2024.
- [34] W. Xu, Y. Cai, D. He, J. Lin, and F. Zhang, "Fast-lio2: Fast direct lidar-inertial odometry," *IEEE Trans. Robot.*, vol. 38, no. 4, pp. 2053–2073, 2022.
- [35] T. Qin, P. Li, and S. Shen, "Vins-mono: A robust and versatile monocular visual-inertial state estimator," *IEEE Trans. Robot.*, vol. 34, no. 4, pp. 1004–1020, 2018.
- [36] T. Qin, S. Cao, J. Pan, and S. Shen, "A general optimization-based framework for global pose estimation with multiple sensors," *arXiv preprint arXiv:1901.03642*, 2019.